Chinese Chemical Letters 33 (2022) 3241–3244

Contents lists available at ScienceDirect

Chinese Chemical Letters

journal homepage: www.elsevier.com/locate/cclet

Wearable membranes from zirconium-oxo clusters cross-linked polymer networks for ultrafast chemical warfare agents decontamination

Litao Ma[a], Jiamin Xie[a], Xiaoshan Yan[b,*], Zhiwei Fan[a], Heguo Li[b], Lin Lu[b], Likun Chen[b], Yi Xin[b], Panchao Yin[a,*]

[a] South China Advanced Institute for Soft Matter Science and Technology & State Key Laboratory of Luminescent Materials and Devices, South China University of Technology, Guangzhou 510641, China
[b] State Key Laboratory of NBC Protection for Civilian, Research Institution of Chemical Defense, Beijing 100191, China

ARTICLE INFO

Article history:
Received 1 September 2021
Revised 8 October 2021
Accepted 19 October 2021
Available online 29 October 2021

Keywords:
Molecular clusters
Chemical warfare agents
Catalysis
Polymer nanocomposites
Wearable devices

ABSTRACT

The urgent need for immediate personal protection against chemical warfare agents (CWAs) spurs the requirement on robust and highly efficient catalytic systems that can be conveniently integrated to wearable devices. Herein, as a new concept for CWA decontamination catalyst design, sub-nanoscale, catalytically active zirconium-oxo molecular clusters are covalently integrated in flexible polymer network as crosslinkers for the full exposure of catalytic sites as well as robust framework structures. The obtained membrane catalysts exhibit high swelling ratio with aqueous content as 84 wt% and therefore, demonstrate quasi-homogeneous catalytic activity toward the rapid hydrolysis of both CWA, soman (GD) ($t_{1/2}$ = 5.0 min) and CWA simulant, methyl paraoxon (DMNP) ($t_{1/2}$ = 8.9 min). Meanwhile, due to the covalent nature of cross-linkages and the high flexibility of polymer strands, the membranes possess promising mechanical strength and toughness that can stand the impact of high gas pressures and show high permeation for both CO_2 and O_2, enabling their extended applications in the field of collective/personal protective materials with body comfort.

Chemical warfare agents (CWAs) represent some of the most toxic compounds ever synthesized in human history, which have been used in the world wars and the recent Syrian civil war, and caused grave harm to humanity and the environment [1,2]. Even during recent years, as representative CWAs, nerve agents, including the most notorious organophosphates, have been frequently used for assassination since they can irreversibly bind to acetylcholinesterase and lead to nerve system dysfunction, respiratory fail and finally asphyxiation in minutes [3,4]. The catalyzed hydrolysis of the labile P-X bond offers a reliable method to detoxify organophosphate-based nerve agents while the design of catalysts have been evolving from solid heterogeneous materials to porous metal-organic frameworks (MOFs) for rapid and stable catalytic kinetics resulting from their high surface area and enriched catalytic sites [1,4–7]. The processabilities of MOF catalysts have been further optimized through their complexation with inorganic or polymeric fibers textiles, or polymer matrices; nevertheless, their catalytic efficiencies could be lowered due to the blockage of MOF pore accessibility by densely packed polymer chains [5,8–11]. Researchers incorporate MOF catalysts on fibers, for example, by electrospinning, dip coating or adhesive bindings, which inevitably lead to catalysts agglomeration or leaching originated from the weak interaction between the complexed phases [10,12,13]. Meanwhile, the increasing interests in wearable devices with convenient fabrication process are projected in the development of next generation CWA decontamination technology to respond to the urgent need for immediate personal protection against CWAs [4,11]. This imposes intense requirements on the facile integration of completed catalytic systems into single device, where CWAs can be rapidly and completely destructed with no need of extra auxiliary substances. Additionally, to facilitate device fabrication, the mechanical performance of the catalysts, an ignored factor in previous studies, needs rational optimization synergized with their enhanced or at least remained catalytic activities. Therefore, the development of catalytic systems with balanced packaging feasibility, mechanical properties, and catalytic performances should be targeted.

* Corresponding authors.
E-mail addresses: yanxiaoshan@gmail.com (X. Yan), yinpc@scut.edu.cn (P. Yin).

https://doi.org/10.1016/j.cclet.2021.10.059
1001-8417/

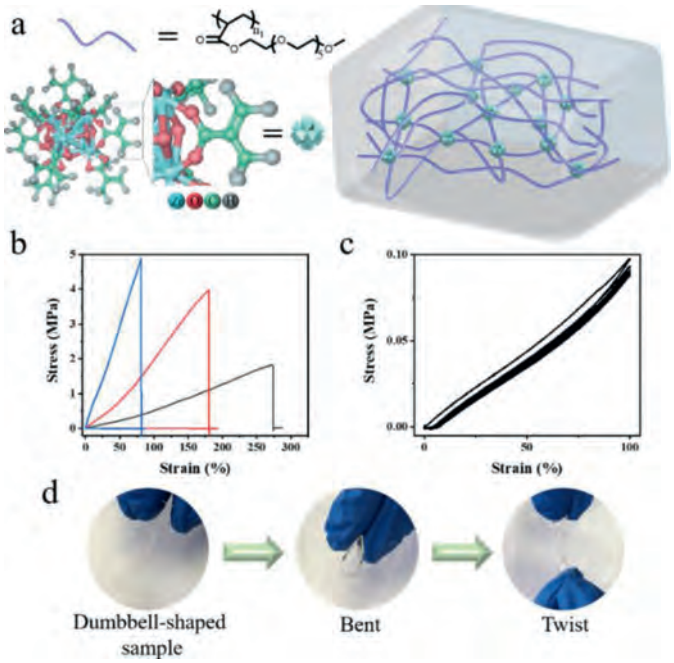

Fig. 1. Mechanical property of PZrCCs. (a) Illustration of polymer nanocomposite integrated by Zr-oxo MCs. (b) Tensile stress-strain curves of PZrCCs-1 (black line), PZrCCs-2 (red line) and PZrCCs-3 (blue line). (c) Five loading-unloading cycles of the PZrCCs-1 without interval. (d) Photographs of PZrCCs in a dumbbell shape with bending and twisting.

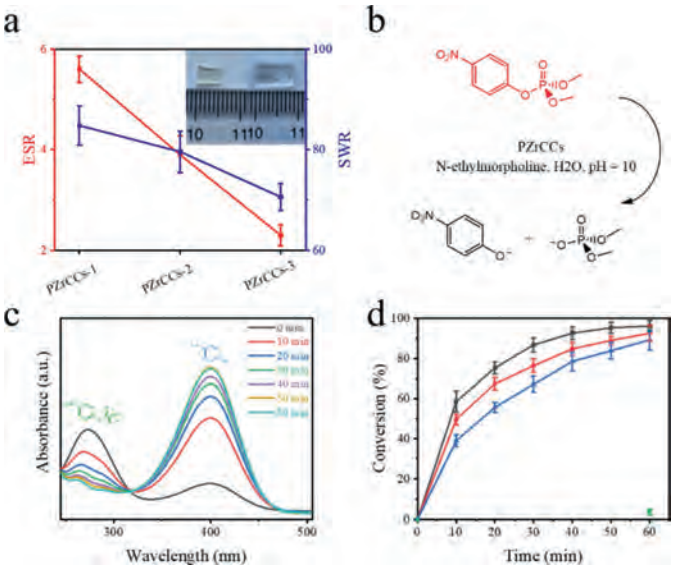

Fig. 2. Solvent trapping and catalytic property of PZrCCs. (a) Solvent capture parameters of PZrCCs in deionized water, in which the left side shows the equilibrium swelling ratio (ESR) and the right side shows the solvent content ratio (SWR) (inset: photograph of before (left) and after (right) swollen state of PZrCCs-2). (b) Reaction conditions for the catalytic decomposition of DMNP using PZrCCs. (c) Ultraviolet-visible monitoring of the formation of *p*-nitrophenoxide. Left peak indicates the wavelength at which DMNP absorbs and right peak indicates the absorbance of *p*-nitrophenoxide, signifying decomposition has occurred. (d) Percentage conversion to *p*-nitrophenoxide versus time for PZrCCs-1 (black), PZrCCs-2 (red), PZrCCs-3 (blue) and background reaction (green). The error bars indicate the standard deviation of three independent catalytic tests.

Polymer nanocomposites (PNCs) allow synergies between the characteristic properties of polymers and nanomaterials and provide great opportunities for the design and facile preparation of multi-functional materials [14–18]. As the major challenge in PNC development, the poor affinity or weak interaction between nanomaterial phase and polymer matrix could lead to phase separation and long-term service failure [19,20]. One widely-recognized solution is to covalently bond nanomaterials with polymer chains, which, however, requires enormous efforts for surface functionalization of nanomaterials [21–23]. Molecular clusters (MCs), as a group of nanoscale atomic assemblies with discrete, well-defined structures, represent the transitional regime between small molecules and colloid nanoparticles (NPs) and thus, demonstrate the convenient surface tailoring capabilities like small molecules and broad functionalities similar to NPs [22,24,25]. PNCs with catalytically active MCs covalently integrated in polymer network demonstrate quasi-homogenous catalytic efficiency and extend the catalysts' applications in flow chemistry and column catalysis [22]. Among MCs, zirconium-oxo clusters possess acidic property and excellent catalytic efficiency for hydrolysis cleavage of phosphate ester, including organophosphate-type nerve agents, originated from hard Lewis acid character of Zr centers [23,26]. Meanwhile, thanks to the well-developed synthetic chemistry of Zr element, Zr-oxo MCs can be designed with various types of hydroxy and/or carboxyl ligands, including acrylates, providing the opportunities to co-polymerize with conventional vinyl monomers [23,27-30]. Herein, we report a series of polymer networks of polyethylene glycol methacrylate (PEGMA) crosslinked by Zr-oxo MCs capped with rich acrylate ligands, which show excellent robustness with toughness of 3.3 MJ/m^3 and possess high gas permeability for both CO_2 and O_2. The PNC networks can swell and trap large amount of aqueous solutions as hydrogels, enabling their quasi-homogeneous and high efficient catalysis toward the hydrolysis destruction of CWAs simulate methyl paraoxon (DMNP, $t_{1/2}$ = 8.9 min) and CWAs of soman (GD, $t_{1/2}$ = 5.0 min)

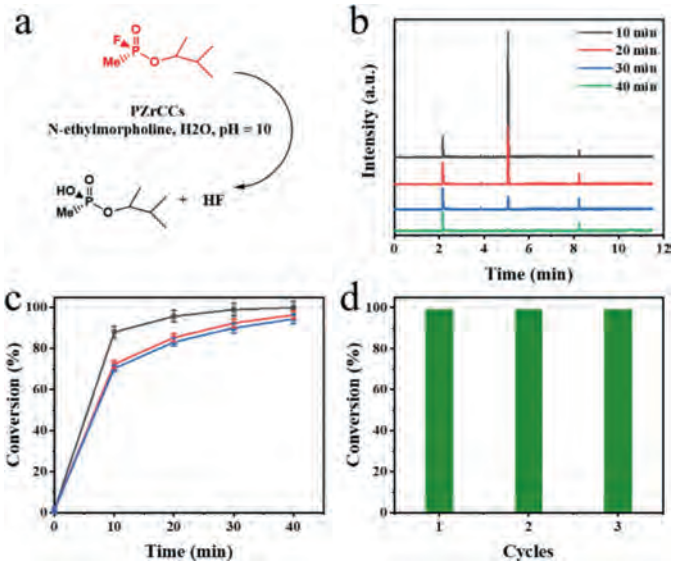

Fig. 3. Evaluation of the catalytic hydrolysis activity of PZrCCs on GD. (a) Reaction conditions for the catalytic decomposition of GD using PZrCCs. (b) Gas chromatography (GC) monitoring of the destruction of GD. Intensity of signal at 5.08 min indicates concentration of GD. (c) Conversion efficiency of GD hydrolysis versus time for PZrCCs-1(black squares), PZrCCs-2 (red circles), PZrCCs-3 (blue triangles). The error bars indicate the standard deviation of three independent catalytic tests. (d) Recycle tests on the catalytic degradation of real CWAs GD base on PZrCCs-1.

with admirable cyclic performances. Without any input of extra auxiliary substances, the rapid and complete destruction of nerve agents can be achieved within the hydrogel catalyst system while the catalysts can be facilely processed into membranes with promising gas permeabilities and mechanical perfor-

mances, facilitating their applications as wearable devices for CWA decontamination.

The PNC catalysts are prepared from the copolymerization of Zr-oxo MCs with conventional vinyl monomers to enable the covalent bonding among MCs and polymer matrix for robustness of the systems. Zr-oxo MC capped with 12 acylate acid ligands ($Zr_6(OH)_4O_4(OMC)_{12}$, OMC = methylacrylic acid) can serve as crosslinking agents to copolymerize with polyethylene glycol methacrylate (PEGMA, Mw = 300 g/mol) for polymer network (polymer zirconium cluster composites, PZrCCs) with high affinity to aqueous solutions (Fig. 1a and Fig. S1 in Supporting information). The loadings of MCs are varied from 3.0 wt% to 8.5 wt% (PZrCCs-1, 3 wt%; PZrCCs-2, 5.5 wt%; PZrCCs-3, 8.5 wt%) for the exploration of PNCs' structure-property relationship in the following mechanical performance, catalytic activity, and gas permeability studies (Table S1 and Fig. S3 in Supporting information). Small angle X-ray scattering studies confirm the molecular and homogeneous distribution of MCs in the PNCs with no indication of the formation of crystalline phase or aggregation of MCs (Fig. S2 in Supporting information). PZrCCs show obvious low glass transition temperature (T_g) at −45 °C and confirm the high mobilities of PEGMA side chains, contributing to the materials' flexibilities (Fig. S4 in Supporting information). The polymer network endows PZrCCs with high elasticity, and the covalently bonded Zr-oxo MCs enhance the modulus and toughness of PZrCCs. With Zr-oxo MCs loading increase, the crosslinking densities of PZrCC networks increase and the elongation ratios decrease from 273.1% to 81.4% while their fracture stress and Young's modulus increase from 1.8 Mpa to 4.9 MPa and 0.5 MJ/m^3 to 7.2 MJ/m^3, respectively (Fig. 1b and Fig. S5 in Supporting information). Due to their robust network structures, PZrCCs show excellent deformability and flexibility with stable cyclability. The hysteresis loop appears in the first cycle of the cyclic tensile curve, mainly originated from the breaking up of hydrogen bonding between segment chains. In the following four cyclic tensile processes, the cyclic tensile curves almost overlap with each other (Fig. 1c). PZrCCs can be conveniently processed into various shapes, such as dumbbell shape, and can be bent, twisted (Fig. 1d). Thanks to their excellent mechanical performances and high mobilities/dynamics polymer chain segments, PZrCCs can withstand long-term pressure impact of 105 kPa and show high gas permeability to both CO_2 and O_2 (Table S2 in Supporting information).

PZrCCs are able to swell in polar solvents to form gels and demonstrate quasi-homogeneous catalytic performance. The PEGMA segments show high affinity to polar solvents and thus, PZrCC networks can swell in polar solvents, including aqueous media, and the equilibrium swelling ratio (ESR) and solvent weight ratio (SWR) of the formed hydrogels are inversely proportional to the crosslinking densities of the network and can reach 5.6 and 84.0 wt%, repectively, for PZrCC with lowest Zr-oxo MCs loading (Fig. 2a). The catalytic active Zr-oxo MCs are homogeneously dispersed in polymer matrix and ESR and SWR are crucial indices to their homogeneous catalytic activities since they reflect the accessibility of substrate molecules in solutions to the catalytic sites of Zr-oxo MCs [22]. The formed hydrogel catalysts of PZrCCs represent completed catalytic systems with both catalysts and reaction solution media integrated and therefore, the catalyzed hydrolysis of CWAs can be achieved by the hydrogels with no need of extra chemicals.

Methyl paraoxon (DMNP), as typical simulant for organophosphate-type nerve agents, are firstly applied to confirm the catalytic activities of PZrCC hydrogels. Catalytic hydrolysis of DMNP is carried out using PZrCCs as hydrogel catalysts in an aqueous buffer solution of *N*-ethylmorpholine at pH 10 (Fig. 2b).

The reaction progress is evaluated by monitoring the increased absorbance at 407 nm, which corresponds to the production of *p*-nitrophenoxide from the hydrolysis of DMNP (Fig. 2c) [10]. The reaction kinetics is indexed as the conversion of DMNP during the reaction course. Within 60-min reaction time, 96%, 92% and 90% DMNP conversion can be observed for PZrCCs-1, PZrCCs-2 and PZrCCs-3 catalyst systems, respectively (Fig. 2d). In contrast, the background reaction is ignorable over the same time course with conversion of 2.6%. PZrCCs-1 possesses the highest ERS and SWR among all PZrCCs (Fig. 2a), leading to the highest catalytic efficiencies with the shortest reaction half-life of 8.9 min. This, actually, is superior to most of the reported Zr-MOF-derived catalysts (Table S3 in Supporting information) [3,9,31,32]. As control studies, pure zirconium-oxo MCs with no polymers and pure polymer network with no MCs are applied, respectively, as catalysts and significantly decreased hydrolysis rates of DMNP are observed (Figs. S6 and S7 in Supporting information), suggesting the synergies of polymer matrices and MCs. The immiscibility of pure Zr-oxo MCs with aqueous solutions contributes to their poor catalytic activities. However, during the catalytic process of PZrCCs, the compatibility of the polymer matrix with aqueous media enables the accessibility of Zr-oxo MCs to the substrates, greatly accelerating the catalytic reaction process. Interestingly, zirconium-oxo MCs are covalently bonded with polymer matrix and therefore, stable catalytic efficiencies can be confirmed with more than 95% conversion in all five cyclic catalytic experiments (Fig. S8 in Supporting information). The robustness of CWA destruction catalyst system is highly appreciated while most of the reported systems face the severer issue of catalyst leaching originated from noncovalent interaction between catalysts and dispersed media [10].

Inspired by their catalysis activity against DMNP, highly toxic nerve agent soman (GD) is further tested to confirm the practical applications of PZrCCs. The destruction of GD using PZrCCs hydrogel catalysts are monitored by gas chromatography (GC) (Figs. 3a and b). The peak at 5.08 min in GC measurements, corresponding to GD species, shows rapid decreasing trend during the reactions, suggesting the rapid destruction of GD (Fig. 3b and Fig. S9 in Supporting information). Quantitatively, the destructive conversions of GD are 99%, 92%, 90% for PZrCCs-1, PZrCCs-2 and PZrCCs-3, respectively, within 30 min reaction time (Fig. 3c). Similar to above DMNP catalysis experiments, PZrCCs-1 still yields the highest catalytic activity with reaction half-life as 5.0 min, which is at the level of ultrafast degradation of GD (Table S4 in Supporting information). More importantly, the PZrCCs-1 catalysts can be recycled and no decay of their catalytic efficiencies can be observed (Fig. 3d). Thanks to their high catalytic activities, promising mechanical properties, and high gas permeabilities, the PZrCCs can be facilely processed into membranes and integrated in regular mask for convenient self-detoxify of CWAs (Fig. S10 in Supporting information).

In summary, thanks to the molecular scale, covalent integration of Zr-oxo MCs into polymer network, PNCs with balanced mechanical properties, gas permeability and catalytic activities are designed for feasible CWA destruction. The PZrCCs can trap reaction solutions and rapidly catalyze DMNP and GD destruction with short half-time of 8.9 min and 5.0 min respectively. Moreover, originated from their robust structures, PZrCCs possess stable and high cyclic mechanical and catalytic performances, providing great promise for protection from CWAs. The strategy of fabricating MCs into polymer networks by covalent bond will offer new opportunities to advance the development of robust wearable devices of gas filter or catalytic membrane to protect against harmful pollutants with required processability and mechanical properties.

Declaration of competing interest

The authors declare no competing financial interest.

Acknowledgments

The work is supported by the National Key Research and Development Program of China (No. 2018YFB0704200), the Project of State Key Laboratory of NBC Protection for Civilian (No. ZKGSG-ZB-20194334), the National Natural Science Foundation of China (Nos. 21961142018 and 51873067) and Natural Science Foundation of Guangdong Province (Nos. 2021A1515012024 and 2021A1515010271). The authors are grateful to the help of Mingxin Zhang for providing model of zirconium clustere.

Supplementary materials

Supplementary material provides the experiment section and structural characterizations of $Zr_6(OH)_4O_4(OMC)_{12}$ and PZrCCs; catalytic performance for DMNP and GD of pure zirconium clusters and pure polymer samples; cyclic catalytic performance for DMNP and GD of PZrCCs; comparison of half-lives of DMNP and GD catalyzed by PZrCCs with other inorganic catalysts. Supplementary material associated with this article can be found, in the online version, at doi:10.1016/j.cclet.2021.10.059.

References

[1] T.G. Grissom, A.M. Plonka, C.H. Sharp, et al., ACS Appl. Mater. Interfaces 12 (2020) 14641–14661.
[2] Y. Hou, H. An, Y. Zhang, et al., ACS Catal. 8 (2018) 6062–6069.
[3] H.B. Luo, A.J. Castro, M.C. Wasson, et al., ACS Catal. 11 (2021) 1424–1429.
[4] J. Dong, H. Lv, X. Sun, et al., Chem. Eur. J. 24 (2018) 19208–19215.
[5] S. Holdren, R. Tsyshevsky, K. Fears, et al., ACS Catal. 9 (2019) 902–911.
[6] G.W. Peterson, G.W. Wagner, J. Porous Mater. 21 (2014) 121–126.
[7] F.A. Son, M.C. Wasson, T. Islamoglu, et al., Chem. Mater. 32 (2020) 4609–4617.
[8] N.S. Bobbitt, M.L. Mendonca, A.J. Howarth, et al., Chem. Soc. Rev. 46 (2017) 3357–3385.
[9] H. Liang, A. Yao, X. Jiao, et al., ACS Appl. Mater. Interfaces 10 (2018) 20396–20403.
[10] J. Zhao, D.T. Lee, R.W. Yaga, et al., Angew. Chem. Int. Ed. 55 (2016) 13224–13228.
[11] D.T. Lee, J. Zhao, G.W. Peterson, et al., Chem. Mater. 29 (2017) 4894–4903.
[12] H. Liang, A. Yao, X. Jiao, et al., ACS Appl. Mater. Interfaces 10 (2018) 20396–20403.
[13] H.F. Barton, A.K. Davis, G.N. Parsons, ACS Appl. Mater. Interfaces 12 (2020) 14690–14701.
[14] C.A. Trickett, A. Helal, B.A. Al-Maythalony, et al., Nat. Rev. Mater. 2 (2017) 1–16.
[15] K.P. Sullivan, W.A. Neiwert, H. Zeng, et al., Chem. Commun. 53 (2017) 11480–11483.
[16] J. Kao, K. Thorkelsson, P. Bai, et al., Chem. Soc. Rev. 42 (2013) 2654–2678.
[17] Z.B. Shifrina, V.G. Matveeva, L.M. Bronstein, Chem. Rev. 120 (2020) 1350–1396.
[18] D. Jung, P. Das, A. Atilgan, et al., Chem. Mater. 32 (2020) 9299–9306.
[19] S. Kango, S. Kalia, A. Celli, et al., Prog. Polym. Sci. 38 (2013) 1232–1261.
[20] S. Choi, S.I. Han, D. Kim, et al., Chem. Soc. Rev. 48 (2019) 1566–1595.
[21] H. Zou, S.H. Wu, A.J. Shen, Chem. Rev. 108 (2008) 3893–3957.
[22] L. Ma, Z. Xu, Y. Chen, et al., ACS Appl. Mater. Interfaces 12 (2020) 38655–38661.
[23] M. Vigolo, S. Borsacchi, A. Sorarù, et al., Appl. Catal. B: Environ. 182 (2016) 636–644.
[24] A. Pinkard, A.M. Champsaur, X. Roy, Acc. Chem. Res. 51 (2018) 919–929.
[25] W.B. Zhang, X. Yu, C.L. Wang, et al., Macromolecules 47 (2014) 1221–1239.
[26] G. Kickelbick, U. Schubert, Chem. Ber. 130 (1997) 473–478.
[27] D. Nam, J. Huh, J. Lee, et al., Chem. Sci. 8 (2017) 7765–7771.
[28] J. Liu, W. Duan, J. Song, et al., J. Am. Chem. Soc. 141 (2019) 12064–12070.
[29] G. Kickelbick, P. Wiede, U. Schubert, Inorg. Chim. Acta 284 (1999) 1–7.
[30] G. Trimmel, S. Gross, G. Kickelbick, et al., Appl. Organomet. Chem. 15 (2001) 401–406.
[31] J.E. Mondloch, M.J. Katz, W.C. Isley Iii, et al., Nat. Mater. 14 (2015) 512–516.
[32] R. Chen, C. Tao, Z. Zhang, et al., ACS Appl. Mater. Interfaces 11 (2019) 43156–43165.